

See discussions, stats, and author profiles for this publication at: <https://www.researchgate.net/publication/51237715>

# Highly Sensitive Detection of Proteins and Bacteria in Aqueous Solution Using Surface-Enhanced Raman Scattering and Optical Fibers

ARTICLE *in* ANALYTICAL CHEMISTRY · JUNE 2011

Impact Factor: 5.64 · DOI: 10.1021/ac200707t · Source: PubMed

---

CITATIONS

61

---

READS

107

5 AUTHORS, INCLUDING:



Claire Gu

University of California, Santa Cruz

161 PUBLICATIONS 1,841 CITATIONS

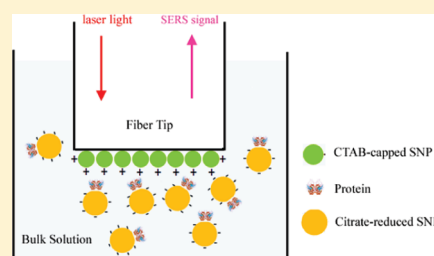
SEE PROFILE

# Highly Sensitive Detection of Proteins and Bacteria in Aqueous Solution Using Surface-Enhanced Raman Scattering and Optical Fibers

Xuan Yang,<sup>†</sup> Claire Gu,<sup>\*,†</sup> Fang Qian,<sup>‡</sup> Yat Li,<sup>‡</sup> and Jin Z. Zhang<sup>\*,‡</sup>

<sup>†</sup>Department of Electrical Engineering and <sup>‡</sup>Department of Chemistry and Biochemistry, University of California, Santa Cruz, California 95064, United States

**ABSTRACT:** We report the detection of the proteins lysozyme and cytochrome *c* as well as the live bacterial cells of *Shewanella oneidensis* MR-1 in aqueous solutions with sensitivities order(s) of magnitude higher than those previously reported. Two highly sensitive surface-enhanced Raman scattering (SERS)-based biosensors using optical fibers have been employed for such label-free macromolecule detections. The first sensor is based on a tip-coated multimode fiber (TCMMF) with a double-substrate “sandwich” structure, and a detection limit of 0.2  $\mu\text{g/mL}$  is achieved in protein detections. The second sensor is based on a liquid core photonic crystal fiber (LCPCF) with a better confinement of light inside the fiber core, and a detection limit of  $10^6$  cells/mL is achieved for the bacteria detection. Both SERS biosensors show great potential for highly sensitive and molecule-specific detection and identification of biomolecules.



Surface-enhanced Raman scattering (SERS) is a promising spectroscopic technique due to its high sensitivity and unique molecular specificity.<sup>1–6</sup> With the strong enhancement of the EM field and the surface chemical enhancement, SERS spectroscopy can provide a nondestructive and ultrasensitive detection down to the single molecule level with intrinsic molecular “fingerprint” information.<sup>7–9</sup> Many studies have successfully demonstrated the great potential of SERS in detections and identifications of a variety of molecules.<sup>10–12</sup>

Due to vital importance in biomedical research, diagnosis, proteomics and microbiology, various biomolecules and systems, including peptides,<sup>13–15</sup> proteins,<sup>16–22</sup> DNA and RNA,<sup>23–25</sup> bacteria,<sup>26–30</sup> tissues,<sup>31,32</sup> and living cells<sup>33,34</sup> have been detected and characterized using SERS previously. However, their complex structures usually make it challenging to carry out direct, label-free SERS detection. In most cases, dye molecules are used as SERS probes for indirect detection of the target analyte molecules of interest.<sup>35–38</sup>

Direct SERS detection of target biological analytes is clearly desired because it simplifies the measurement. In particular, direct detection in aqueous solution is even more preferred because of the characteristics of high reproducibility and in situ measurement capability. However, the SERS signal in direct aqueous solution detection is often weak because of the small polarizability of most biological molecules compared with dye probe molecules.

One solution to this problem is to improve the sensitivity of the detection system. For example, Ozaki et al. reported that by using acidified sulfate as an aggregation agent, proteins can be identified rapidly in solutions, and a detection limit of 5  $\mu\text{g/mL}$  for the protein sample of lysozyme was achieved.<sup>19</sup> Another example is a recent study from our lab,<sup>30</sup> in which both silver

nanoparticles (SNPs) and silver nanowires were applied simultaneously to enhance the SERS signal, and a detection limit of  $10^8$  cells/mL was achieved for the bacteria *Shewanella*, which is a Gram-negative facultative anaerobe with extracellular electron transfer capability<sup>39</sup> that has various applications in bioremediation of contaminated and radioactive soils,<sup>40</sup> heavy metal detoxification,<sup>41</sup> and microbial fuel cells.<sup>42</sup> Both cases demonstrated that SERS can be applied directly in aqueous solution detection; however, more efforts are still needed to improve the sensitivity of these detection systems.

While SERS offers unique molecular selectivity and high sensitivity, optical fibers have been used as SERS probes because of their flexibility, compactness, reliability, and in situ remote sensing capability.<sup>43–51</sup> Previously, we demonstrated that fiber SERS probes, such as the tip-coated multimode fiber (TCMMF) probe<sup>47</sup> and liquid core photonic crystal fiber (LCPCF) probe,<sup>49</sup> can provide higher sensitivity than bulk solution detections. TCMMF is based on a double-substrate “sandwich” structure utilizing the stronger EM field between the SNPs coated on the fiber tip and the ones in the solution to enhance the signal, and LCPCF is based on the confinement of the excitation/Raman scattered light and the analyte inside the fiber core to increase the effective interaction volume. However, the “sandwich” effect in our previous TCMMF probe was relatively weak as a result of the small size of the SNPs coated on the fiber tip and the same type of charges (negatively charged) carried by these two types of SNPs.<sup>47</sup> Moreover, the SERS performance of TCMMF and LCPCF probes was evaluated using mainly small dye molecules;

**Received:** March 20, 2011

**Accepted:** June 21, 2011

**Published:** June 21, 2011

fewer efforts have been devoted to studying these probes' applications in the detection of interesting biological macromolecules.

In this paper, we report the detection of the proteins lysozyme and cytochrome *c* as well as the bacteria *Shewanella oneidensis* MR-1 in aqueous solutions with sensitivities order(s) of magnitude higher than those previously reported.<sup>19,30</sup> This high sensitivity has been achieved with two types of SERS-based biosensors using optical fibers. The first fiber SERS sensor that consists of a new TCMMF probe with positively charged SNPs coated on the fiber tip is fabricated and demonstrated in aqueous protein SERS detections, with negatively charged SNPs mixed in the solution. This oppositely charged double-substrate "sandwich" effect is demonstrated, for the first time, in aqueous protein detection. The detection limit of the two protein samples, lysozyme and cytochrome *c*, both reported in previous SERS studies,<sup>14,18–21</sup> has reached as low as 0.2  $\mu\text{g/mL}$ .

The second fiber SERS sensor consists of a highly sensitive LCPCF probe, employed in the bacteria SERS detection. The detection limit using the LCPCF for *S. oneidensis* has reached down to  $10^6$  cells/mL, 3 orders of magnitude lower than that obtained from the direct detection of the same sample in the bulk solution. Both types of optical fiber SERS sensors offer promising platforms for highly sensitive label-free detections and characterizations of biological macromolecules in aqueous solutions.

## EXPERIMENTAL SECTION

**Chemicals.** Lysozyme and cytochrome *c* were purchased from Sigma-Aldrich. Milli-Q water was used throughout the present study.

**Bacterial Strain and Culture Conditions.** *S. oneidensis* MR-1 strain (ATCC 700550) was purchased from the American Type Culture Collection (ATCC, Manassas, VA). The MR-1 cells were cultured in lactate-defined minimum medium, which consists of (per liter of deionized water) 20 mM sodium lactate, 28 mM  $\text{NH}_4\text{Cl}$ , 1.34 mM KCl, 5 mM  $\text{NaH}_2\text{PO}_4$ , 0.7 mM  $\text{Na}_2\text{SO}_4$ , 1 mM  $\text{MgSO}_4 \cdot 7\text{H}_2\text{O}$ , 20 mM PIPES, 52 mM NaCl, 0.2 mM  $\text{CaCl}_2$ , 1 mL vitamin, and 1 mL trace metal elements. Cells were grown aerobically at 30 °C in a water bath incubator with vigorous shaking at 150 rpm.

**Preparation of Silver Colloid.** The SNPs used in the sample solution were synthesized using the Lee and Meisel protocol, which used silver nitrate as the metal precursor and sodium citrate as the reducing agent.<sup>52</sup> The ones coated on the fiber tip were cetyltrimethylammonium bromide (CTAB)-capped SNPs, which were prepared by a one-step reaction in an ethanol/water system.<sup>53</sup> Basically, CTAB ethanol solution (2 mL, 1 mM) was mixed with aqueous silver nitrate solution (30 mL, 5 mM) under vigorous stirring. After 10 min, freshly prepared aqueous sodium borohydride solution (1%) was added as the reducing agent until the color of the mixed solution changed to yellow-green and the color did not change when more sodium borohydride was added. One milliliter of the prepared CTAB-capped SNPs was purified by centrifugation (14 000 rpm, 25 min), and the solid SNPs were redispersed into 1 mL of Milli-Q water and ready for coating. Formations of both the citrate-reduced negatively charged SNPs and the CTAB-capped positively charged SNPs were monitored by UV–vis spectroscopy using a HP 8452A spectrometer with 2 nm resolution. The size of the citrate-reduced SNPs was determined using a transmission electron microscope (TEM, model JEOL JEM 1200EX).

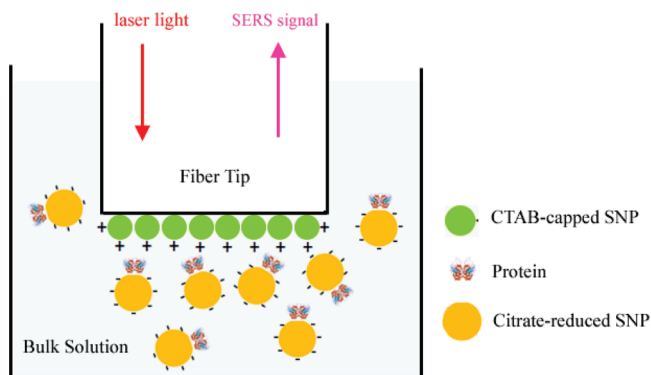


**Figure 1.** Schematic of the TCMMF SERS probe in aqueous protein detection.

**Preparation of SERS Substrates and Fiber Probes.** For aqueous protein SERS detection, the bulk sample preparation was the same as that reported by Ozaki et al.<sup>19</sup> Briefly, the protein samples were diluted 1/10 with the aggregation agent (0.1 M  $\text{Na}_2\text{SO}_4$ , pH = 3) and then were mixed with the citrate-reduced SNPs (1:5, v/v). The fiber used for the TCMMF SERS probe was purchased from Newport (model F-MLD-500). The preparation of this fiber SERS probe was simply performed by dipping one cleaved end into CTAB-capped SNP solution for 3 h. Scanning electron microscopy (SEM, model FEI Quanta 3D FEG dual beam SEM) was used to observe the size and distribution of the SNPs coated on the fiber tip.

For aqueous bacteria of *Shewanella* SERS detection, the bacteria samples were simply mixed with the citrate-reduced SNPs (1:9, v/v). The fiber used for the LCPCF SERS probe was purchased from Crystal Fiber A/S (model AIR-6-800) and prepared as previously.<sup>49</sup> Briefly, a 5 cm hollow core photonic crystal fiber (HCPCF) segment was cut carefully at both ends, and a fusion splicer (model FITEL S175) was used to seal all the cladding holes at both ends.

**SERS Measurements.** The SERS signals were collected using a Renishaw Raman System (Renishaw Inc., model RM2000) with a 632.8 nm excitation light. The laser power was around 2 mW, and the exposure time for each SERS measurement was 10 s. In a bulk detection, the laser excitation light was directly focused onto the sample solution. During detection with a TCMMF SERS probe, the coated end of the TCMMF was dipped into the mixed sample solution, and the other end was placed under the microscope for coupling between the fiber and the laser light and collecting the SERS signal, as well.<sup>47</sup> During a detection with a LCPCF SERS probe, one sealed end of the HCPCF was dipped into the solution and then placed under the microscope for measurements.<sup>49</sup> All the SERS spectra represented in this study were baseline-corrected.

## RESULTS AND DISCUSSION

Figure 1 illustrates the schematic of the TCMMF SERS probe with an oppositely charged double-substrate "sandwich" structure operating in aqueous protein detections. In this study, we developed a new coating strategy by using the CTAB-capped positively charged SNPs to coat the fiber tip. Compared with the previous method,<sup>47</sup> CTAB-capped SNPs have a relatively larger size (25 nm vs 5 nm) and an opposite charge with respect to the SNPs in the bulk solution. The electrostatic force from the

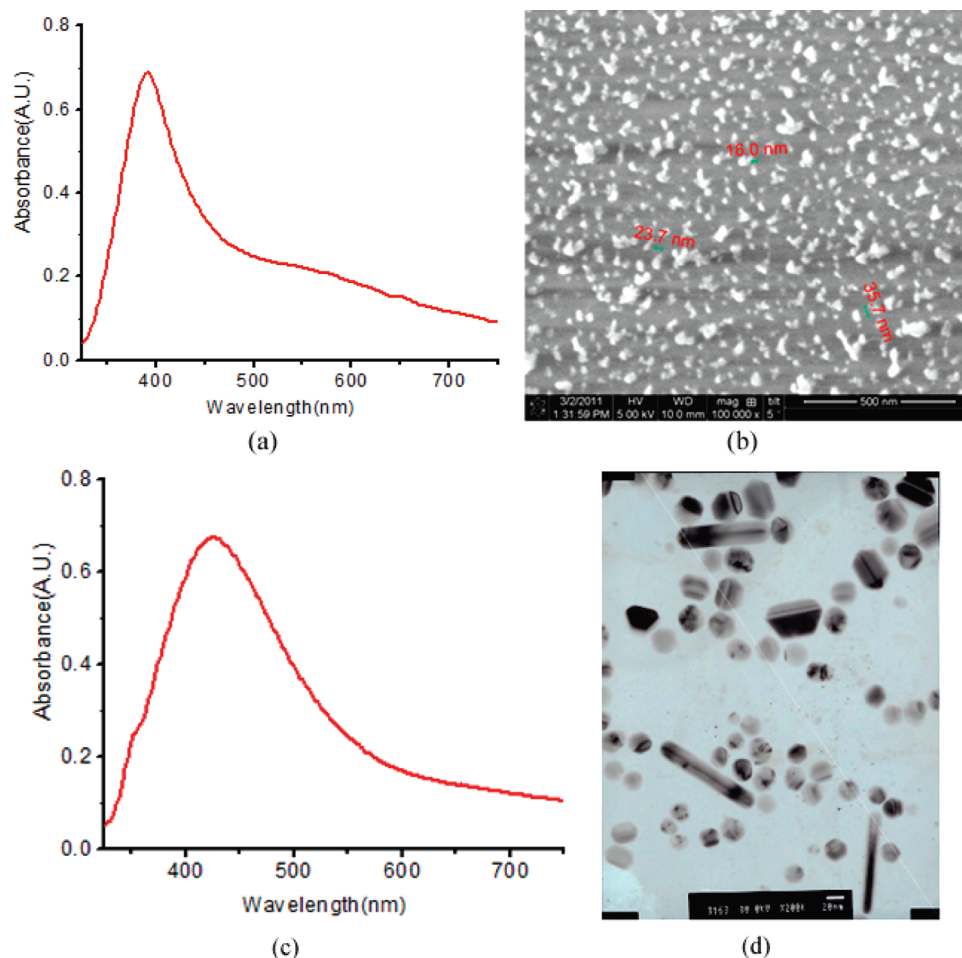


**Figure 2.** (a) UV–vis of CTAB-capped SNPs with the surface plasmon resonance at 391 nm; (b) SEM image of the CTAB-capped SNPs coated on the fiber end. (c) UV–vis of citrate-reduced SNPs with the surface plasmon resonance at 424 nm; (d) TEM image of the citrate-reduced SNPs.

oppositely charged surface can decrease the gap distance between these two types of SNPs, therefore facilitating the formation of the “sandwich” structure. Since the EM field between the SNPs increases when the gap distance decreases, the shorter gap distance can lead to a stronger EM field and, therefore, an increased SERS signal. Moreover, both the synthesis and coating of CTAB-capped SNPs are much easier and highly reproducible. The synthesis is a one-step reaction without complex procedures. The coating can be easily achieved with dip-coating for a relatively short time period because of the electrostatic force between the negatively charged silica surface of the fiber and the positively charged surface of the SNPs. Figure 2a shows the UV–vis spectrum of the CTAB-capped SNPs with a surface plasmon resonance (SPR) at 391 nm. Figure 2b shows the SEM image of the SNPs coated on the fiber tip with an average size of 25 nm and a uniform coating density of 400 particles/ $\mu\text{m}^2$ . The UV–vis spectrum and the TEM image of the citrate-reduced SNPs are also provided in Figure 2c,d, which shows a SPR at 424 nm and an average size of 30 nm.

Due to the stronger EM field introduced by the double-substrate “sandwich” structure, the TCMMF SERS probe can detect a lower concentration in aqueous protein solution. As shown in Figure 3 and Figure 4 respectively, while the detection limit of lysozyme (one type of protein with no chromophore) and cytochrome *c* (one type of hemoproteins) by bulk detection

is 2  $\mu\text{g}/\text{mL}$ , which is similar to the 5  $\mu\text{g}/\text{mL}$  reported previously in aqueous solution detection,<sup>19</sup> the TCMMF can achieve a detection limit of 0.2  $\mu\text{g}/\text{mL}$ , which is 1 order of magnitude lower than the bulk detection. This detection limit is also comparable and even a little lower than that using the dried protein–silver film strategy proposed by Culha et al.<sup>21</sup> Compared with the dried film strategy, our TCMMF probe in aqueous solution detection can offer several unique advantages: high reproducibility, flexibility, and also in situ remote sensing capability. Moreover, we recently demonstrated that the TCMMF SERS probe can be easily integrated with a portable Raman system while preserving the higher sensitivity,<sup>51</sup> which shows great potential for more practical applications in protein detections and characterizations outside the laboratory.

For both bulk solution and TCMMF detections, the SERS spectra of lysozyme and cytochrome *c* are in good agreement with the previously reported literature.<sup>14,19,21</sup> Table 1 provides the band assignments for these two proteins. For the spectra of lysozyme as shown in Figure 3, major Raman peaks are observed at 765 (Trp), 1359 (Trp), 1442 ( $\text{CH}_2$  scissoring), 1508 (Phe, His, Trp), and 1646  $\text{cm}^{-1}$  (amide I). In the TCMMF scheme, an additional strong peak at 1304  $\text{cm}^{-1}$  was observed and can be assigned to  $\text{CH}_2$  wagging mode. In addition, it is noticed that some of the peaks get different signal enhancements when using the TCMMF. On average, the signal enhancement is around



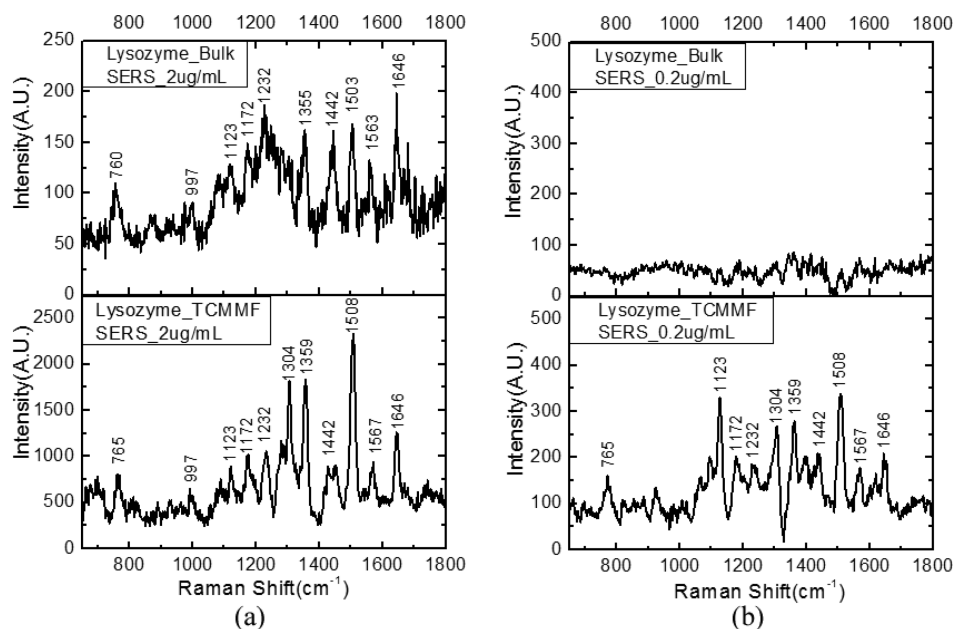


**Figure 3.** SERS spectra of lysozyme detected by bulk solution and TCMMF probe at various concentrations: (a) 2  $\mu\text{g/mL}$ ; (b) 0.2  $\mu\text{g/mL}$ .

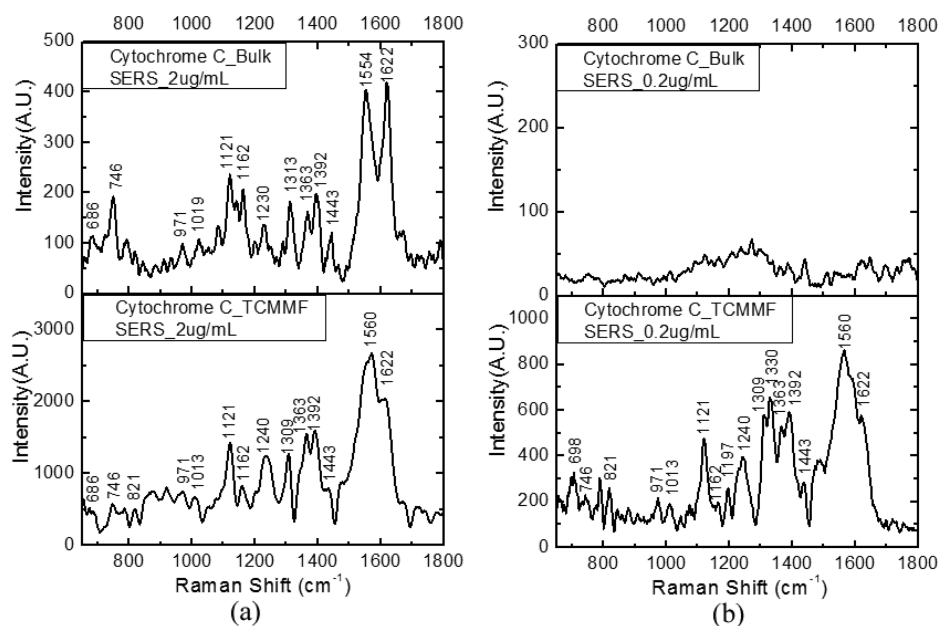


**Figure 4.** SERS spectra of cytochrome *c* detected by bulk solution and TCMMF probe at various concentrations: (a) 2  $\mu\text{g/mL}$ ; (b) 0.2  $\mu\text{g/mL}$ .

10 times for lysozyme. However, the signal enhancement for the 1508  $\text{cm}^{-1}$  peak is  $\sim 18$  times, and that for the 1442  $\text{cm}^{-1}$  peak is  $\sim 5$  times. Both the new emerging peak and different signal enhancements for different peaks in TCMMF are mainly due to the redistribution of EM field by the double-substrate “sandwich” structure. For example, the strongest EM field associated with a single nanoparticle is near the surface, and the strongest EM field associated with a dimer system is inside the gap. Some segments of the protein that are not the closest to the surface of the citrate-reduced SNPs can lie in the gap, which leads to a much stronger enhancement. Depending on their positions in the new SERS substrate, the SERS signal enhancements can therefore be different. With this additional information, it can

help us better understand the adsorption of the protein on the metal surface.

For the spectra of cytochrome *c* shown in Figure 4, major Raman peaks are observed at 1121 ( $\text{NH}_3^+$  deformation), 1230 (amide III), 1313 ( $\text{CH}_2$  wag), 1363 (Trp), 1392 ( $\text{COO}^-$  symmetric stretching), 1554 (Trp), and 1622  $\text{cm}^{-1}$  (amide I). Similar to what occurred in lysozyme detection, some new peaks are observed at 821, 1197, and 1330  $\text{cm}^{-1}$  and can be attributed to Try; Try and Phe; and Trp, respectively. In addition, the sensitivity enhancement varies for different peaks, with an average enhancement factor of 7.

Although the TCMMF SERS probe works well with the nanometer-scale protein molecules and can push the sensitivity

1 order of magnitude higher than the bulk detection, it is challenging to directly apply the TCMMF for the micrometer-scale systems, such as bacteria of *Shewanella* (size:  $2\ \mu\text{m} \times 0.5\ \mu\text{m} \times 0.5\ \mu\text{m}$ ). The reason is that the large target analytes sandwiched between the SNPs create a large gap between the SNPs and thereby reduce the effective EM enhancement. One possible scheme might be to make the SNPs on the inner wall of the bacteria inside the solution,<sup>26</sup> and therefore, when applying the TCMMF probe, the wall of the bacteria can be sandwiched between the SNPs instead of the whole molecule. However, in this study, we are focusing on mixing the SNPs directly with the sample solution, in which the SNPs are physically attached on the outer wall of the bacteria. Therefore, instead of using the TCMMF probe, we found that the LCPCF probe developed

**Table 1. Band assignments for lysozyme and cytochrome c:**

lysozyme	cytochrome c	band assignments
	686, 698	same as reported <sup>17,19</sup>
760, 765	746	Trp
	821	Try
	971	C–C stretching
997	1019, 1013	Phe
1123	1121	NH <sub>3</sub> <sup>+</sup> deformation
1172	1162	Try
	1197	Try + Phe
1232	1230, 1240	amide III
1304	1313, 1309	CH <sub>2</sub> wagging
	1330	Trp
1355, 1359	1363	Trp
	1392	COO <sup>−</sup> symmetric stretching
1442	1443	CH <sub>2</sub> scissoring
1503, 1508		Phe, His, Trp
1563, 1567	1554, 1560	Trp
1646	1622	amide I

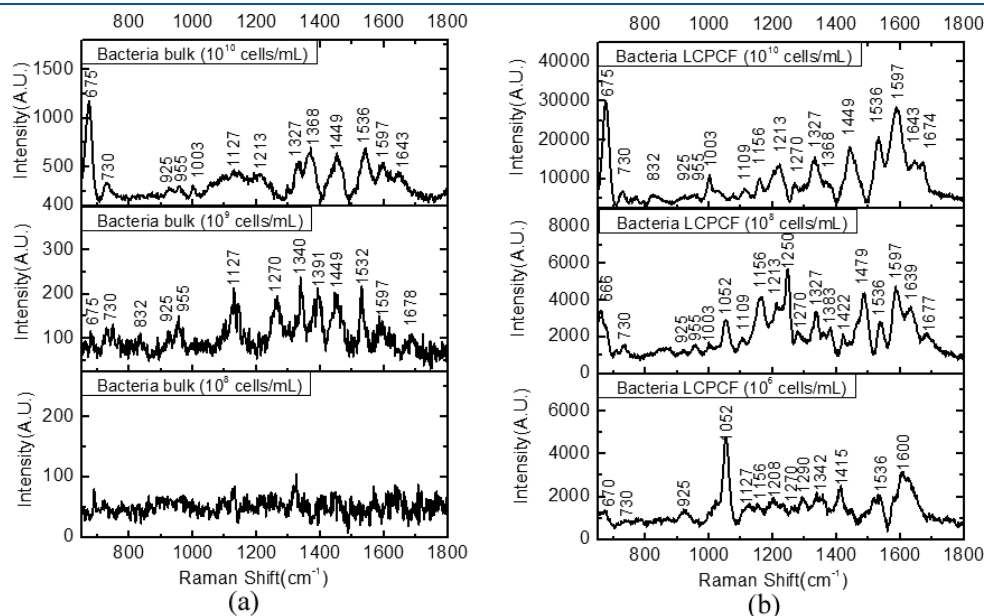
by our group<sup>49</sup> can significantly reduce the detection limit of *Shewanella* cells. In an LCPCF, the central core of the fiber (diameter:  $6\ \mu\text{m}$ ) is filled with the sample solution due to the capillary force, while the laser excitation/Raman scattering light is well guided in the core due to both the photonic bandgap effect and the higher refractive index of the liquid inside the core.<sup>49</sup> Therefore, the effective volume for the sample solution to interact with the excitation light is increased, and the SERS signal can be enhanced significantly.

Figure 5 shows the SERS spectra of MR-1 cells obtained in bulk detection and using the LCPCF SERS probe at various concentrations. Compared with a detection limit of  $10^9$  cells/mL in bulk detection, the LCPCF pushes the detection limit down to  $10^6$  cells/mL. At the same high concentration of  $10^{10}$  cells/mL, the sensitivity enhancement is around 30 times, choosing one of the major peaks at  $1449\ \text{cm}^{-1}$  as a reference, which is generally consistent with our previous results using Rhodamine 6G as a test molecule for the LCPCF SERS probe.<sup>49</sup>

Table 2 summarizes the tentative band assignments for the SERS spectra of MR-1 cells.<sup>14,27–30,54</sup> Some of the major Raman peaks come from the CH<sub>2</sub> wagging mode ( $1327\ \text{cm}^{-1}$ ) and scissoring mode (1368, 1449, and  $1479\ \text{cm}^{-1}$ ).<sup>14</sup> Other major Raman peaks can be assigned to the COO<sup>−</sup> asymmetric stretching mode ( $1536\ \text{cm}^{-1}$ ),<sup>14</sup> bacterial amide ( $1597\ \text{cm}^{-1}$ ),<sup>54</sup> and amide I ( $1643$  and  $1674\ \text{cm}^{-1}$ ).<sup>14</sup>

Control SERS experiments of the lactate medium without the bacteria were performed both in bulk detection and using the LCPCF probe and are shown in Figure 6. It should be noticed that at low concentrations, peaks from the lactate medium or lactate medium/LCPCF can be observed:  $1340$  and  $1391\ \text{cm}^{-1}$  were observed in bulk detection and peaks at  $1052$ ,  $1342$ , and  $1383\ \text{cm}^{-1}$  were observed in LCPCF detection, respectively.

Considering that the enhanced schemes of both TCMMF and LCPCF can be applicable to macromolecule SERS detection in aqueous solution, the possibility of combining the effects in both sensors might be interesting to explore for further enhancing the



**Figure 5.** SERS spectra of MR-1 cells detected by (a) bulk detection ( $10^{10}$ ,  $10^9$ ,  $10^8$  cells/mL) and (b) using the LCPCF probe ( $10^{10}$ ,  $10^8$ ,  $10^6$  cells/mL), respectively.

Table 2. Band Assignments for Bacteria of *S. oneidensis* MR-1

bulk ( $10^{10}$ cells/mL)	bulk ( $10^9$ cells/mL)	LCPCF ( $10^{10}$ cells/mL)	LCPCF ( $10^8$ cells/mL)	LCPCF ( $10^6$ cells/mL)	assignments
675	675	675	666	670	same as reported <sup>26</sup>
730	730	730	730	730	adenine
	832	832			CCH (aliphatic)
925	925	925	925	925	C—COO <sup>−</sup> stretching
955	955	955	955		C—C stretching
1003		1003	1003		Phe
			1052	1052	lactate medium in LCPCF
		1109	1109		
1127	1127			1127	NH <sub>3</sub> <sup>+</sup> deformation
		1156	1156	1156	NH <sub>3</sub> <sup>+</sup> deformation
1213		1213	1213	1208	ring breath
	1270	1270	1250, 1270	1270, 1290	amide III
1327		1327	1327		CH <sub>2</sub> wagging
	1340			1342	lactate medium
1368		1368			CH <sub>2</sub> scissoring
	1391		1383		lactate medium
			1422	1415	COO <sup>−</sup> symmetric stretching
1449	1449	1449	1479		CH <sub>2</sub> scissoring
1536	1532	1536	1536	1536	COO <sup>−</sup> asymmetric stretching
1597	1597	1597	1597	1600	bacterial amide
1643		1643	1639		amide I
	1678	1674	1677		amide I

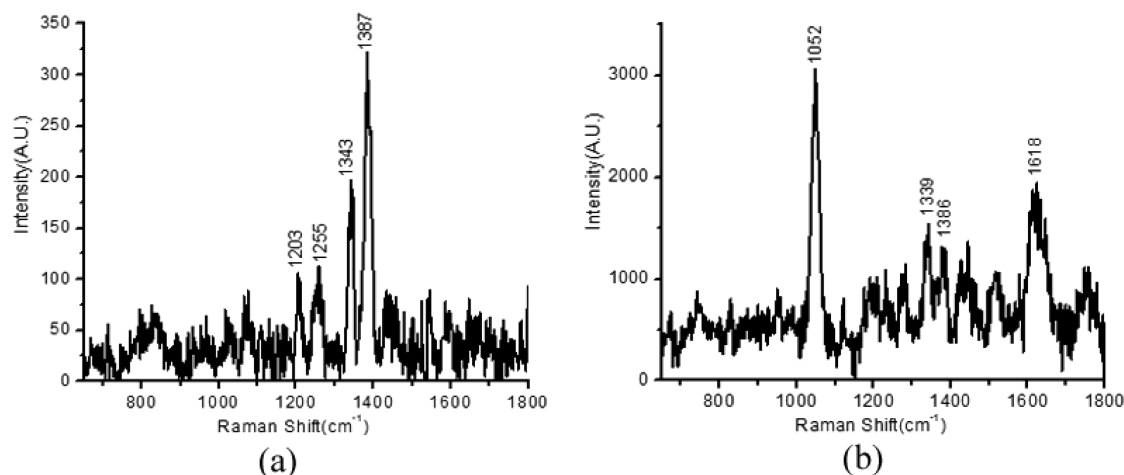


Figure 6. Control experiment with lactate medium and SNPs but without MR-1 cells (a) in bulk detection and (b) using the LCPCF SERS probe.

sensitivity of the detection, for example, a probe structure similar to the protocol of the inner wall coated LCPCF demonstrated by our group previously.<sup>48</sup> Therefore, there is clearly room for further improving the sensor architecture and sensitivity.

## CONCLUSION

In summary, we have reported the detections of the proteins lysozyme and cytochrome *c* as well as the bacteria *S. oneidensis* MR-1 in aqueous solutions with sensitivities order(s) of magnitude higher than those previously reported. At the same time, we have demonstrated two highly sensitive fiber SERS sensors for label-free macromolecule detections in aqueous solution. The TCMMF SERS probe is demonstrated,

for the first time, for the double-substrate “sandwich” effect in aqueous protein detections, and a detection limit of 0.2  $\mu\text{g/mL}$  is achieved for two protein samples, lysozyme and cytochrome *c*. The LCPCF SERS probe is employed for the detection of *Shewanella* bacteria and has pushed the detection limit from  $10^9$  to  $10^6$  cells/mL. High sensitivity, flexibility, and also in situ remote sensing capability make these fiber probes promising platforms in practical applications of label-free SERS detections of biomolecules.

## AUTHOR INFORMATION

### Corresponding Author

\*E-mails: [claire@soe.ucsc.edu](mailto:claire@soe.ucsc.edu) (C.G.); [zhang@ucsc.edu](mailto:zhang@ucsc.edu) (J.Z.).

## ■ ACKNOWLEDGMENT

We acknowledge support from the National Science Foundation (NSF), ECCS-0823921. Y.L. acknowledges financial support of this work in part by NSF, CBET-1034222. We thank Damon Wheeler in the Department of Chemistry and Biochemistry and Changhui Mao in the Department of Molecular, Cell and Developmental Biology at the University of California, Santa Cruz for their assistance in the SEM experiment and the calculation of bacteria concentration, respectively.

## ■ REFERENCES

- (1) Campion, A.; Kambhampati, P. *Chem. Soc. Rev.* **1998**, 27, 241–250.
- (2) Kneipp, K.; Kneipp, H.; Itzkan, I.; Dasari, R. R.; Feld, M. S. *J. Phys.: Condens. Matter* **2002**, 14, R597–R624.
- (3) Otto, A.; Mrozek, I.; Grabhorn, H. *J. Phys.: Condens. Matter* **1992**, 4, 1143–1212.
- (4) Moskovits, M. *Rev. Mod. Phys.* **1985**, 57, 783–826.
- (5) Chang, R. K.; Furtak, T. E. *Surface Enhanced Raman Scattering*; Plenum Press: New York, 1982.
- (6) Schwartzberg, A. M.; Zhang, J. Z. *J. Phys. Chem. C* **2008**, 112, 10323–10337.
- (7) Nie, S.; Emory, S. R. *Science* **1997**, 275, 1102.
- (8) Kneipp, K.; Wang, Y.; Kneipp, H.; Perelman, L. T.; Itzkan, I.; Dasari, R. R.; Feld, M. S. *Phys. Rev. Lett.* **1997**, 78, 1667.
- (9) Wang, Z.; Pan, S.; Krauss, T. D.; Du, H.; Rothberg, L. J. *Proc. Natl. Acad. Sci. U.S.A.* **2003**, 100, 8638–8643.
- (10) Lee, S.; Kim, S.; Choo, J.; Shin, S. Y.; Lee, Y. H.; Choi, H. Y.; Ha, S.; Kang, K.; Oh, C. H. *Anal. Chem.* **2007**, 79, 916–922.
- (11) Ruan, C.; Wang, W.; Gu, B. *Anal. Chem.* **2006**, 78, 3379–3384.
- (12) Cozar, O.; Leopold, N.; Jelic, C.; Chis, V.; David, L.; Mocanu, A.; Tomoaia-Cotisel, M. *J. Mol. Struct.* **2006**, 788, 1–6.
- (13) Herne, T. M.; Ahern, A. M.; Garrell, R. L. *J. Am. Chem. Soc.* **1991**, 113, 846–854.
- (14) Stewart, S.; Fredericks, P. M. *Spectrochim. Acta, Part A* **1999**, 55, 1615–1640.
- (15) Mitchell, B. L.; Patwardhan, A. J.; Ngola, S. M.; Chan, S.; Sundararajan, N. *J. Raman Spectrosc.* **2008**, 39, 380–388.
- (16) Han, X. X.; Jia, H. Y.; Wang, Y. F.; Lu, Z. C.; Wang, C. X.; Xu, W. Q.; Zhao, B.; Ozaki, Y. *Anal. Chem.* **2008**, 80, 2799–2804.
- (17) Wang, M.; Benford, M.; Jing, N.; Cote, G.; Kameoka, J. *Microfluid. Nanofluid.* **2009**, 6, 411–417.
- (18) Han, X. X.; Kitahama, Y.; Itoh, T.; Wang, C. X.; Zhao, B.; Ozaki, Y. *Anal. Chem.* **2009**, 81, 3350–3355.
- (19) Han, X. X.; Huang, G. G.; Zhao, B.; Ozaki, Y. *Anal. Chem.* **2009**, 81, 3329–3333.
- (20) Han, X. X.; Zhao, B.; Ozaki, Y. *Anal. Bioanal. Chem.* **2009**, 394, 1719–1727.
- (21) Kahraman, M.; Sur, I.; Culha, M. *Anal. Chem.* **2010**, 82, 7596–7602.
- (22) Delfino, I.; Bizzarri, A.; Cannistraro, S. *Biophys. Chem.* **2005**, 113, 41–51.
- (23) Bell, S. E. J.; Sirimuthu, N. M. S. *J. Am. Chem. Soc.* **2006**, 128, 15580–15581.
- (24) Culha, M.; Stokes, D.; Allain, L. R.; Vo-Dinh, T. *Anal. Chem.* **2003**, 75, 6196–6201.
- (25) Cao, Y. C.; Jin, R.; Mirkin, C. A. *Science* **2002**, 297, 1536–1540.
- (26) Efrima, S.; Bronk, B. V. *J. Phys. Chem. B* **1998**, 102, 5947–5950.
- (27) Zeiri, L.; Bronk, B. V.; Shabtai, Y.; Eichler, J.; Efrima, S. *Appl. Spectrosc.* **2004**, 58, 33–40.
- (28) Jarvis, R. M.; Brooker, A.; Goodacre, R. *Anal. Chem.* **2004**, 76, 5198–5202.
- (29) Chu, H.; Huang, Y.; Zhao, Y. *Appl. Spectrosc.* **2008**, 62, 922–931.
- (30) Preciado-Flores, S.; Wheeler, D. A.; Tran, T. M.; Tanaka, Z.; Jiang, C.; Barboza-Flores, M.; Qian, F.; Li, Y.; Chen, B.; Zhang, J. Z. *Chem. Commun.* **2011**, 47, 4129–4131.
- (31) Aydin, O.; Kahraman, M.; Kilic, E.; Culha, M. *Appl. Spectrosc.* **2009**, 63, 662–668.
- (32) Aydin, O.; Altas, M.; Kahraman, M.; Bayrak, O. F.; Culha, M. *Appl. Spectrosc.* **2009**, 63, 1095–1100.
- (33) Kneipp, J.; Kneipp, H.; Wittig, B.; Kneipp, K. *Nanomed. Nanotechnol. Biol. Med.* **2010**, 6, 214–226.
- (34) Tang, H. W.; Yang, X. B. B.; Kirkham, J.; Smith, D. A. *Appl. Spectrosc.* **2008**, 62, 1060–1069.
- (35) Cao, Y. C.; Jin, R.; Nam, J.-M.; Thaxton, C. S.; Mirkin, C. A. *J. Am. Chem. Soc.* **2003**, 125, 14676–14677.
- (36) Grubisha, D. S.; Lipert, R. J.; Park, H.-Y.; Driskell, J.; Porter, M. D. *Anal. Chem.* **2003**, 75, 5936–5943.
- (37) Gong, J. L.; Liang, Y.; Huang, Y.; Chen, J. W.; Jiang, J. H.; Shen, G. L.; Yu, R. Q. *Biosens. Bioelectron.* **2007**, 22, 1501–1507.
- (38) Han, X. X.; Kitahama, Y.; Tanaka, Y.; Guo, J.; Xu, W. Q.; Zhao, B.; Ozaki, Y. *Anal. Chem.* **2008**, 80, 6567–6572.
- (39) Caccavo, F., Jr.; Blakemore, R. P.; Lovley, D. R. *Appl. Environ. Microbiol.* **1992**, 58, 3211–3216.
- (40) Myers, C. R.; Neelson, K. H. *Science* **1988**, 240, 1319–1321.
- (41) Zhao, J.-S.; Manno, D.; Thiboutot, S.; Ampleman, G.; Hawari, J. *Int. J. Syst. Evol. Microbiol.* **2007**, 57, 2155–2162.
- (42) Biffinger, J. C.; Byrd, J. N.; Breanna, L. D.; Ringeisen, B. R. *Biosens. Bioelectron.* **2008**, 23, 820–826.
- (43) Zhang, Y.; Gu, C.; Schwartzberg, A. M.; Zhang, J. Z. *Appl. Phys. Lett.* **2005**, 87, 123105.
- (44) Stokes, D. L.; Vo-Dinh, T. *Sens. Actuators, B* **2000**, 69, 28–36.
- (45) Stokes, D. L.; Chi, Z. H.; Vo-Dinh, T. *Appl. Spectrosc.* **2004**, 58, 292–298.
- (46) Polwart, E.; Keir, R. L.; Davidson, C. M.; Smith, W. E.; Sadler, D. A. *Appl. Spectrosc.* **2000**, 54, 522–527.
- (47) Shi, C.; Yan, H.; Gu, C.; Ghosh, D.; Seballos, L.; Chen, S.; Zhang, J. Z. *Appl. Phys. Lett.* **2008**, 92, 103107.
- (48) Shi, C.; Lu, C.; Gu, C.; Tian, L.; Newhouse, R.; Chen, S.; Zhang, J. Z. *Appl. Phys. Lett.* **2008**, 93, 153101.
- (49) Yang, X.; Shi, C.; Wheeler, D.; Newhouse, R.; Chen, B.; Zhang, J. Z.; Gu, C. *J. Opt. Soc. Am. A* **2010**, 27, 977–984.
- (50) Yang, X.; Wang, D.; Zhu, J.; Gu, C.; Zhang, J. Z. *Chem. Phys. Lett.* **2010**, 495, 109–112.
- (51) Yang, X.; Tanaka, Z.; Newhouse, R.; Xu, Q.; Chen, B.; Chen, S.; Zhang, J. Z.; Gu, C. *Rev. Sci. Instrum.* **2010**, 81, 123103.
- (52) Lee, P. C.; Meisel, D. *J. Phys. Chem.* **1982**, 86, 3391.
- (53) Patil, V.; Malvankar, R. B.; Sastry, M. *Langmuir* **1999**, 15, 8197–8206.
- (54) Sengupta, A.; Mujacic, M.; Davis, E. J. *Anal. Bioanal. Chem.* **2006**, 386, 1379–1386.